

Visualization of Two-dimensional Flows by a Liquid (Soap) Film Tunnel

Gharib, M.*¹ and Beizaie, M.*²

*¹ California Institute of Technology, 1200 East California Boulevard, Pasadena, CA 91125, USA.

*² University of California, 9500 Gilman Pr., La Jolla, San Diego, CA 92093-0411, USA.

Received 17 February 1999.
Revised 15 June 1999.

Abstract: Experimentally produced two-dimensional flows have become possible in recent years due to the invention of Liquid Film Tunnel (LFT) in 1987 by Gharib and Derango. This simple, inexpensive, yet powerful device, which we have improved extensively over the last decade, can generate a variety of flows. Liquid (soap) films can be visualized through light interference effects produced by small variations in the film thickness. Flow-disturbing objects such as cylinders, wedges, and air bubbles create these variations. Monochromatic visualization of these thickness variations will render phenomenally accurate graphic information about the flow patterns thus produced. Under a polychromatic light, these interference effects can be spectacular, due to reflection of different colors by different isothickness regions.

Keywords: liquid (soap) film tunnel (LFT), two-dimensional flow, refraction.

1. Introduction

Liquid films, especially those made out of surfactant solutions, have long been nominated as good media for the production and study of two-dimensional hydrodynamics (Mysels, Shinoda, and Frankel, 1959; Frankel and Mysels, 1969; Mysels and Frankel, 1978; Rusanov and Krotov, 1979; Couder, 1981; Couder, Chomaz, and Rabaud, 1989). These films; usually called soap films, although a surfactant is not necessarily a soap; are very thin, self-sustained fluid layers in which hydrodynamical experiments can be done. In such a film, the velocity field is confined to its surface and is practically two-dimensional. As was suggested ingeniously by Mysels and demonstrated in excellent series of experiments by Couder, soap films are good candidates for the simulation of two-dimensional flows. However, since soap films age with time, the experiments that involve still films suffer from several shortcomings. The observation periods are short and the films do not maintain a uniform mean thickness with time, which makes quantitative flow measurements difficult.

In an effort to avoid such shortcomings, a continuously flowing liquid film tunnel (LFT) was invented in 1987 (Gharib and Derango, 1989), and used by us to study a variety of two-dimensional flows (Beizaie and Gharib, 1997; Gharib and Beizaie, 1991). This LFT, which has undergone considerable improvement since its invention, consists of a wire frame one end of which is positioned in a diluted surfactant mixture while the other end is subjected to either of two film-pulling mechanisms (Fig. 1). The frame is constructed of 1/8" rods of either copper or steel.

The main portion of the LFT is a horizontal frame section consisting of two parallel rods (Fig. 1a). Two legs support this flat section, one at each end. The liquid films are pulled by the shearing action of a two-dimensional water jet, which is produced by flow of water through a rectangular opening, mounted on a horizontal pipe. By rotating this pipe, the shearing angle can be changed and by varying the water flow rate one can vary the pulling

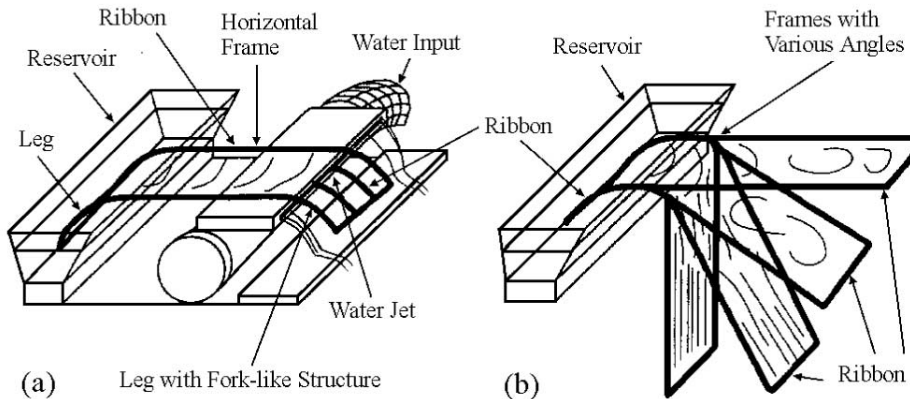


Fig. 1. The liquid film tunnel (LFT), driven by a running water sheet (a), or gravity (b); the thick lines represent fine cloth ribbons glued on top of the frames.

force. Note that the leg at the film/water jet interface has fork-like structures. These structures help to stabilize the film/water jet interface.

The size of the frame is limited by the horizontal film's tendency to bow at the flat section of the tunnel. The maximum width of the frame to avoid this effect is 4". In the horizontal version of LFT, the stream-wise length of the horizontal test section can be extended up to 1.5 ft without greatly reducing the life of the film. Several other factors, including dry air, severe ventilation, vibration and unsteadiness or turbulence in the water jet can shorten the film life. Fine cloth ribbons are glued to the top of the frame to help prevent rupture of the liquid films due to water evaporation. So, the films are actually supported by these thin wet ribbons rather than by the rods themselves. Therefore, the menisci along the ribbons have a constant thickness, independent of the surfactant concentration. The horizontal films are also quite uniform in overall thickness when running steadily undisturbed. However, the overall film thickness is a function of the surfactant concentration, higher concentrations producing thinner films. The local thickness varies due to disturbances such as stretching, thinning, or foreign objects piercing it. These thickness variations are visible due to reflection of different colors by different isothickness regions.

With a steady water jet in the horizontal version, and in the absence of severe ventilation and vibration, the films can run for hours, provided that a fresh surfactant mixture is added to the reservoir continuously.

In our experiments, we also tried a totally vertical frame with the surfactant solution running over it. Although this appeared like a fast running LFT, close examinations revealed the existence of extremely large-scale non-uniformities in the background flow and thickness (similar to the second version with angle greater than 45°). Since we could not improve the flow conditions for non-horizontal cases, we did not continue this line of experiments. However, a group at the University of Pittsburgh has recently reported some success with application of vertical liquid films (Rutgers et al., 1996).

2. Visualization

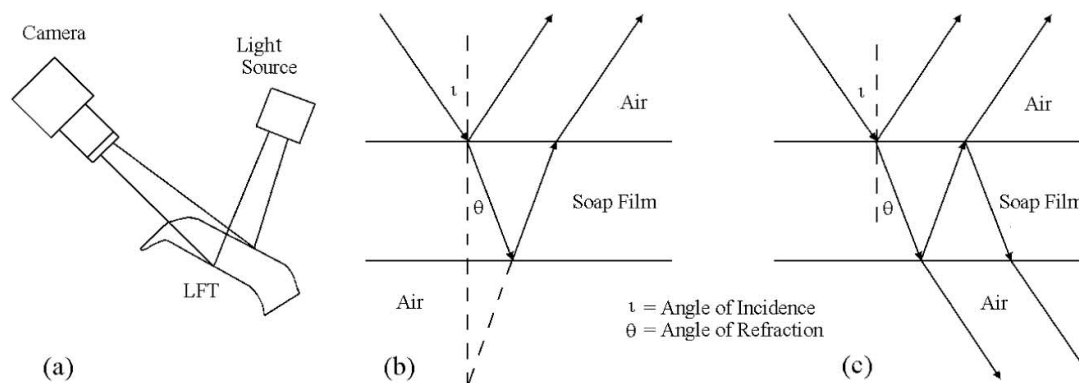
Liquid (soap) films can be visualized through light interference effects produced by small variations in the film thickness. Such variations are generated during pulling of the film from the reservoir due to gravitational effects, and further downstream by the disturbing foreign objects such as cylinders, strips, and air bubbles. Monochromatic visualization of these thickness variations will render phenomenally accurate graphic information about the flow patterns thus produced. Under a polychromatic light, these interference effects can be spectacular, due to reflection of different colors by different isothickness regions.

The colors that are produced on soap films by interference of white light have fascinated scientists for more than a century (Plateau, 1873; Gibbs, 1876; Boys, 1890). Lawrence (1929) published one of the earliest mathematical works relating these colors to the film thickness. For a soap film with refractive index $\mu = 1.41$, he found the following results for normally incident white light. Each film thickness t listed below should be multiplied by $\cos \theta$ if the incident light has an angle of refraction θ .

Mysels, Shinoda, and Frankel (1959) and Isenberg (1978), analyzed the physics of soap-film visualization. They noted that light reflected from a soap film reaches the eye (or camera) primarily by two routes. One route is reflection at the upper surface of the soap film (with air) and the other is reflection at the lower surface (with

Table 1. Soap film color-thickness data calculated by Lawrence (1929).

Observed Color	t , microns	Observed Color	t , microns	Observed Color	t , microns
<i>First Order</i>					
Black	0.0060	Purple	0.3960	Green	0.7900
Silvery	0.0120	Blue	0.4100	Green	0.8420
<i>Second Order</i>					
Violet	0.2160	Blue	0.4280	Pink	0.8930
Blue	0.2500	Emerald Green	0.4660	Pink	0.9450
Green	0.2900	Yellow Green	0.5020	<i>Sixth Order</i>	
Yellow	0.3220	Carmine	0.5420	Green	1.0000
Orange	0.3480	Bluish Red	0.5780	Green	1.0440
<i>Crimson</i>					
	0.3710	<i>Fourth Order</i>		Pink	1.1000
		Grass Green	0.5970	Pink	1.1500
		Green	0.6340	<i>Seventh Order</i>	
		Yellow Green	0.6820	Green	1.2100
		Carmine	0.7460	Green	1.2650
				Pink	1.3150
				Pink	1.3700
				<i>Eighth Order</i>	
				Green	1.4200
				Pink	1.5000

Fig. 2. Schematics of the optical paths: (a) general view, (b) reflection at, and (c) transmission through a liquid film; in either case, the incident light undergoes an optical path difference of $2\mu t \cos \theta$.

interstitial liquid) followed by refraction through the upper; see Fig. 2. Since the second route has undergone a refraction at the upper surface after beginning in air, it will have an optical path difference of $2\mu t \cos \theta$ with the first route. To this we must add a half-wavelength, $\lambda/2$, due to the additional phase difference of π that occurs at the air-film interface.

The two reflected beams join to produce a combined beam which reaches the observer and whose intensity depends on the optical path difference. If the difference of path retards one of the wave trains by a full number of wavelengths, so that the crests of one coincide with the crests of the other, the two beams are in phase and so interfere constructively giving an intense reflection. Conversely, if the difference of path retards one of the wave trains by an additional half wavelength, so that the crests of one coincide with the troughs of the other, the two beams are 180° out of phase. They will thus interfere destructively to cancel each other and give a reflection which is less than the sum of the two and may even be zero. This complete cancellation requires that the intensities of the two reflections be equal. In soap films, this is indeed the case, because of the equality of the two changes in refractive index.

This nearly complete lack of reflection from a very thin film gives it a black appearance (when viewed against a black background) in sharp contrast with the magnificent colored reflections from the thicker film. For this reason the term "black film" is applied to such films. It should not be taken to imply a lack of transparency; on

the contrary, it results from almost complete transparency with essentially no reflection.

As the thickness of a film increases, the intensity of its reflection first increases from zero to a maximum, which occurs for each color when the thickness reaches its quarter wavelength and then decreases. When the thickness is about a quarter of the wave-length of the average color, the reflected light is approximately balanced - as the long wave-lengths have not yet reached their maximum and the short ones have passed it - so that the reflection is essentially white, the film is called "silvery." As the thickness increases further this balance is destroyed and individual colors predominate in turn and the rainbow-colored film appears. When the thickness becomes much larger, reinforcement and cancellation occur repeatedly across the spectrum and again a balanced, white reflection is obtained. By using an unbalanced light source with prominent spectral lines, or better monochromatic light, one can however follow the periodic reinforcements and cancellations up to a quite large thickness. In this way fringes given by films with thickness of the order of 50 wavelengths, i.e. 25 microns or 1/40 mm can be seen. The relation between the reflected intensity, I , refractive index, μ , film thickness, t , angle of refraction, θ , and wavelength, λ , is (Isenberg, 1978)

$$I = I_0 \sin^2(2\pi\mu t \cos \theta / \lambda). \quad (1)$$

Equation (1) shows that with increasing the film thickness, the reflected intensity varies sinusoidally between a minimum of zero and a maximum value, I_0 . If the first thickness at which this greatest reflected intensity occurs is denoted by t_o , the reflected intensity may be expressed as

$$I = I_0 \sin^2(\pi t / 2t_o). \quad (2)$$

The thickness of first maximum reflection, t_o , depends on the wave-length within the film, hence on the color of light and on the refractive index of the film, and also on the direction of incidence of the light. The average of the above expression over a wide range of film thickness, or of wavelength, is $I_0/2$, which is equal to the sum of the two reflection intensities from single surfaces.

3. Case Studies

In this section, several examples of flows observed on our LFT are displayed. These are common cases, observed under monochromatic or polychromatic (white) light. The types of flows generated on LFT are not limited to these examples; many other configurations are possible as far as the imagination of future researchers will go.

3.1 Undisturbed Horizontal Flow

The undisturbed, horizontal liquid (soap) films, are quite uniform in thickness, as evident even better under monochromatic light; see Fig. 3. By optical techniques (Isenberg, 1978), the maximum film thickness variation

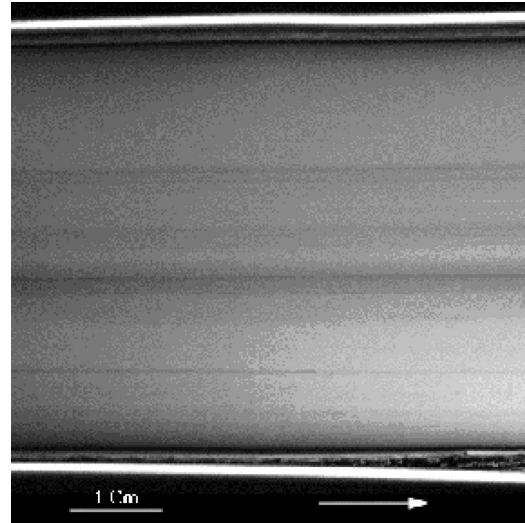


Fig. 3. A typical undisturbed soap film produced by the liquid film tunnel.

between two consecutive fringe patterns can be calculated as

$$\delta = \lambda / (2\mu \cos \theta). \quad (3)$$

For a typical horizontal film, this is estimated to be in the order of 100 nm for a 5 micron thick film lit by monochromatic green light of 500 nm wavelength. Usually, the distance between such fringes in the horizontal section is about 5 to 10 cm. Therefore, the horizontal section of the film is uniform in thickness by an error less than 0.0002%.

The image in Fig. 3 was captured by a Pulnix TM 9701 CCD video camera, under a low-pressure sodium light with an effective wavelength of about 590 nm.

3.2 Laminar and Turbulent Jets

The jets were produced by running the films through a pair of rods that formed a two-dimensional nozzle in a 6 cm-wide plain frame. This nozzle had a fixed inlet of about 4 cm width and an adjustable outlet. Figure 4a shows a 1.5 mm (6 cm/sec) laminar jet in a 4 μm -thick film made out of a 1.0% surfactant mixture. The large growth rate observed in this image is due to the lower surface tension within the jet, which had a Reynolds number of about 25. Figure 4b shows a turbulent jet on the same frame, using the same surfactant mixture, but with a narrower opening (1.0 mm) and a higher velocity (200 cm/sec), producing a Reynolds number of about 500. In both cases, the velocity of the co-flow (the main film) was about 20-25 cm/sec.

These images were taken by a Nikon photographic camera, under GE's Daylight fluorescent light.

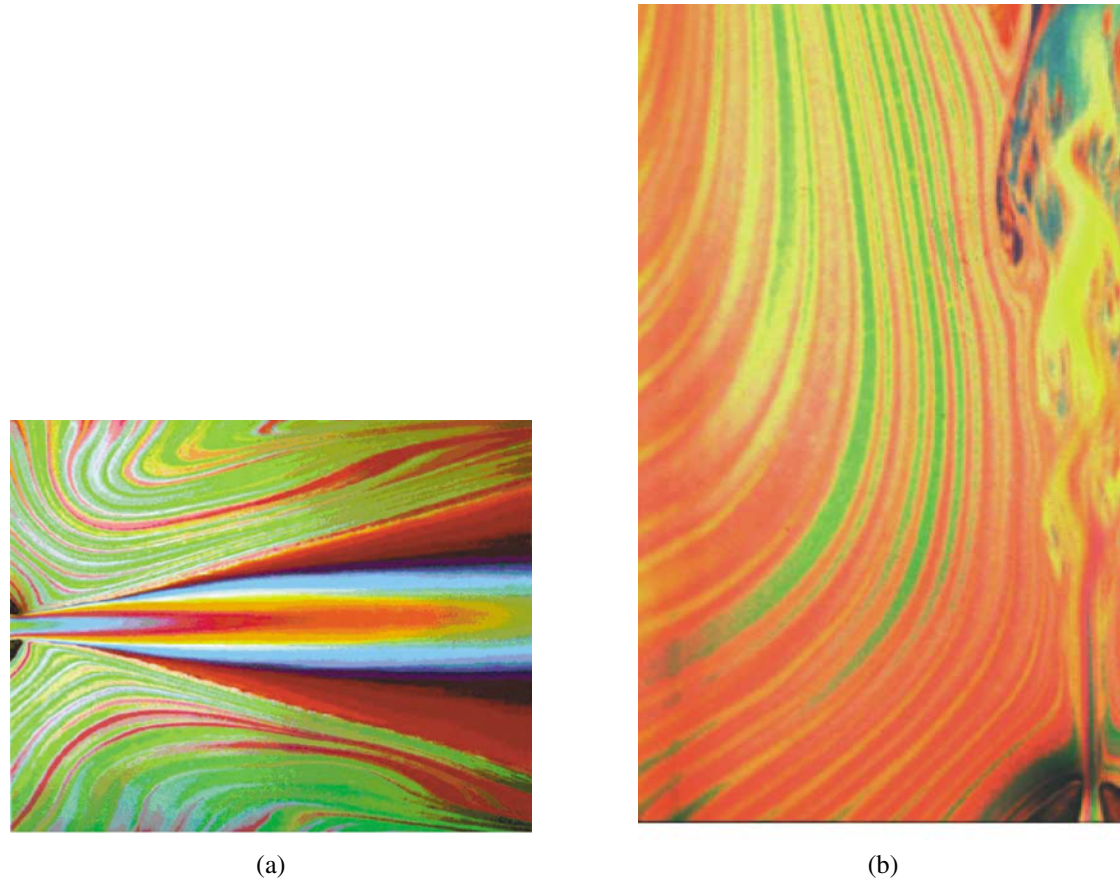


Fig. 4. A laminar jet with $\text{Re} = 25$ (a) and a turbulent jet with $\text{Re} = 500$ (b) in a soap film produced by the LFT.

3.3 Grid Turbulence

Figure 5 includes monochromatic pictures of two-dimensional grid turbulence in a 4-cm wide liquid film at an area about 3 mm ($x/d = 1$) downstream from the grid. The film was produced by a 0.5% surfactant mixture and run at about 20-30 cm/sec through an array of 1.4-mm diameter rods spaced 3.2 mm center to center, producing a Reynolds number of about 110 (a) or 150 (b). The undisturbed film thickness was estimated to be about 7 μm .

These images were captured by a Pulnix TM 9701 CCD video camera, under a low-pressure sodium light (590 nm).

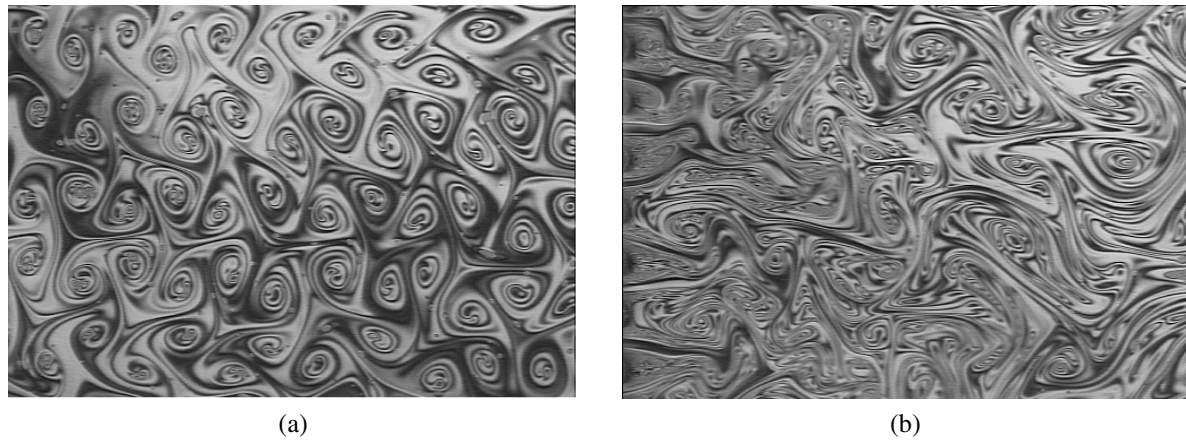


Fig. 5. Two-dimensional grid turbulence at $x/d = 1$; (a) $\text{Re} = 110$, (b) $\text{Re} = 150$.

3.4 Wake

Figure 6a demonstrates a steady wake pattern behind a 0.5-mm steel cylinder. In Fig. 6b we see a Karman vortex street behind a 6-mm-wide copper strip piercing a soap film in our LFT. The soap film was produced by a 0.65vol% solution, running on a plain, horizontal frame with a flat section of 20 cm by 4 cm. The undisturbed film velocity at centerline was 20-30 cm/sec, and its thickness about 5 microns. With an estimated kinematic viscosity of 0.0375 cm^2/sec , this translates to a Reynolds number of 25 (a) or 480 (b).

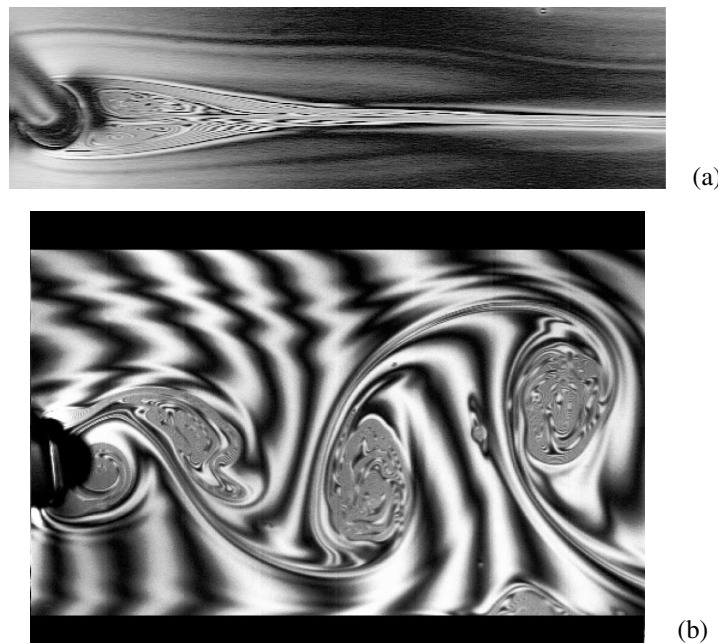


Fig. 6. Two-dimensional wake with a Reynolds number of 25 (a), and 480 (b).

The image in Fig. 6a was taken by a Pulnix TM 9701 CCD video camera, and the one in Fig. 6b by a 1000 frame/sec Kodak EktaPro video camera. In both cases illumination was by a low-pressure sodium light (590 nm).

3.5 Sink Flow

Figure 7 depicts a 2D sink in a liquid (soap) film made out of a 1.0% surfactant mixture. The maximum velocity in this 7-mm-wide sink was about 120 cm/sec. The undisturbed (on a plain frame) film thickness was estimated to be about 4 μm , and its velocity measured about 20 cm/sec. The observed streamlines produce a model for blood flow through a ruptured mitral valve. They provide direct confirmation of convergence geometries for comparison with the ultrasonic Doppler studies in these same geometries.

This image was taken by a Canon FT photographic camera, under GE's Soft White fluorescent light.

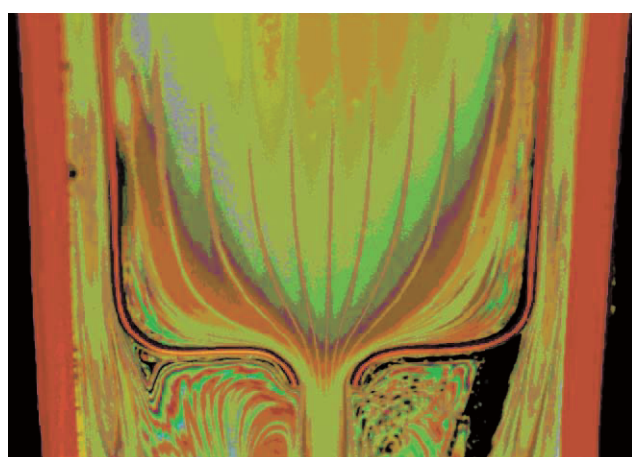


Fig. 7. A two-dimensional sink.

Acknowledgments

The authors wish to thank Professor Karol Mysels for his valuable advice and encouragement. This work was supported by National Science Foundation (NSF Contract MSM 88-20182) at University of California, San Diego.

References

- Beizaie, M. and Gharib, M., Fundamentals of a Liquid (Soap) Film Tunnel, *Experiments in Fluids*, 23 (1997), 130-140.
- Bluestein, B.R. and Hilton, C.L., *Amphoteric Surfactants*, (1982), Marcel Dekker, New York, 5, 178, 268.
- Boys, C.V., *Soap Bubbles*, (1890), Society for Promoting Christian Knowledge, London.
- Chirash, W., Liquid Light-Duty Detergents, *Journal of American Oil Chemists Society*, 58 (1981), 362A-366A.
- Couder, Y., The Observation of a Shear Flow Instability in a Rotating System with a Soap Membrane, *Journal of Physics Letters*, 42 (1981), L429-L431.
- Couder, Y., Chomaz, J.M. and Rabaud, M., On the Hydrodynamics of Soap Films, *Physica*, D 37 (1989), 384-405.
- Cross, J., *Nonionic Surfactants-Chemical Analysis*, (1977), Marcel Dekker, New York, 4.
- Doi, J., *Album of Visualization*, 12 (1995), The Visualization Society of Japan, Tokyo, 1.
- Frankel, S. and Mysels, K.J., The Bursting of Soap Films, II, Theoretical Considerations. *Journal of Physical Chemistry*, 73 (1969), 3028-3038.
- Gharib, M. and Beizaie, M., A Novel Soap-Film Tunnel for Studying Two-Dimensional Flows, *Proceedings of the Sixth International Symposium on Flow Visualization (Yokohama)*, (1991-10), 233-237.
- Gharib, M. and Derango, P., A Liquid Film (Soap-Film) Tunnel to Study Two-Dimensional Laminar and Turbulent Shear Flows, *Physica*, D 37 (1989), 406-416.
- Gibbs, J.W., *The Collected Works of*, (1931), Longmans Green, New York. [originals dating 1876 and 1878].
- Hibi, K., *Album of Visualization*, 13 (1996), The Visualization Society of Japan, Tokyo, Cover.
- Isenberg, C., *The Science of Soap Films and Soap Bubbles*, (1978), Tieto, Clevedon.
- Lawrence, A.S.C., *Soap Films, a Study of Molecular Individuality*, (1929), Bell, London.
- Mysels, K.J. and Frankel, S., The Effect of a Surface-Induced Gradual Viscosity Increase upon the Thickness of Entrained Liquid Films and the Flow in Narrow Channels, *Journal of Colloid Interface Science*, 66 (1978), 166-172.
- Mysels, K.J., Shinoda, K. and Frankel, S., *Soap Films: Studies of their Thinning and a Bibliography*, (1959), Pergamon, New York.
- Plateau, J., *Statique Experimentale et Theorique des Liquides soumis aux Seules Forces Moleculaires*, (1873), Gauthier-Villars, Paris.
- Rutgers, M.A., Wu, X-L., Bhagavatula, R., Peterson, A.A. and Goldberg, W.I., *Physics of Fluids*, 8 (1996), 2847.
- Rusanov, A.I. and Krotov, V.V., Gibbs Elasticity of Liquid Films, Threads, and Foams, *Progress in Surface and Membrane Science*, 13 (1979), 415-524.
- Schick, M.J., *Nonionic Surfactants-Physical Chemistry*, (1987), Marcel Dekker, New York, 821.

Authors' Profiles

Mory Gharib: He is a professor of aeronautics at the California Institute of Technology. He holds a Ph.D. from Caltech, and has made numerous contributions to the understanding of fluid physics through invention of novel experimental techniques such as Digital Particle Image Velocimetry. According to his students, his love for fluid mechanics is contagious. He is well known in the fields of vortex dynamics, cardiovascular flows, free surface phenomena, and image processing.



Masoud Beizaie: He is a research associate at the Center of Excellence for Advanced Materials, University of California, San Diego. He holds a Ph.D. from Syracuse University and is a registered Professional Chemical Engineer. His research interests include image processing, polymers, surfactants, and filtration.